In Vivo Detection of Malignant Thymic Masses by Indium-111-DTPA-D-Phe^1-Octreotide Scintigraphy

Secondo Lastoria, Emilia Vergara, Giovannella Palmieri, Wanda Acampa, Paola Varrella, Corradina Caracò, Raffaele A. Bianco, Pietro Muto and Marco Salvatore

Department of Nuclear Medicine National Cancer Institute, Fondazione G. Pascale, Naples; Center for Nuclear Medicine, Consiglio Nazionale delle Ricerche, Naples; and Department of Molecular and Clinical Oncology and Endocrinology, University Federico II, Naples, Italy

Many tumors with neuroendocrine characteristics express high amounts of somatostatin receptors that enable in vivo imaging with [^{111}In-DTPA-D-Phe^1]-octreotide. In this study, we have analyzed the feasibility in detecting and characterizing thymic masses by somatostatin receptor scintigraphy (SRS). **Methods:** Eighteen patients (13 women, 5 men, ages 18–78 yr; mean ± s.d. = 42.1 ± 17.6 yr) were enrolled in this study. Eleven patients were studied during diagnosis and seven during routine follow-up. In seven patients, myasthenia gravis was the presenting symptom. SRS was performed within 4 wk after CT and/or MRI. Planar and tomographic images were acquired within 24 hr after the injection of approximately 111 MBq of [^{111}In-DTPA-D-Phe^1]-octreotide. The scintigraphic results were categorized according to the histologic findings. **Results:** Histology diagnosed 10 mixed epithelial/lymphoid thymomas (8 with prevalent epithelial component), 2 thymic carcinomas, 1 thymic carcinoid, 1 lymphangioma and 4 thymic hyperplasias. Two thymoma were Stage I, 3 were Stage II, 2 were Stage III and 5 were Stage IV, as was the thymic carcinoid. Indium-111-DTPA-D-Phe^1-octreotide concentrated in primary and/or metastatic sites of thymic tumors, thereby enabling successful external gamma imaging of sites greater than 1.5 cm in size. Tumor-to-lung (T/L) ratios were as high as 7.6-fold (range 1.7–7.6). Untreated thymomas showed higher T/L (4.34 ± 1.57) than treated ones (2.68 ± 1.18). No uptake was detectable in the four patients with benign thymic hyperplasia and the patient with the lymphangioma. **Conclusion:** Indium-111-DTPA-D-Phe^1-octreotide is avidly concentrated within thymic tumors, but it is not concentrated by thymic hyperplasia, which allows differential diagnosis. Thus, in patients with myasthenia gravis, SRS may have a role in characterizing thymic masses, thereby overcoming the limits of cross-sectional imaging modalities.

Key Words: thymoma; indium-111-octreotide; somatostatin receptors; myasthenia gravis

J Nucl Med 1998; 39:634–639

Human thymoma is a rare tumor that usually develops within the anterior mediastinum and may often infiltrate adjacent thoracic organs. However, it rarely metastasizes outside the chest (*1,2*). Thymomas are epithelial tumors frequently associated with an exuberant lymphoid component (*3*), which is usually constituted by immature cortical thymocytes proliferating at rates comparable to those observed in the fetal thymus (*4*). The microenvironmental organization is abnormal in thymomas, and it differs from the normal thymus for the prevalence of cortical areas and the deficiency of medullary ones (*5*). Phenotypic abnormalities, including elevated expression of high-molecular weight cytokeratins and modifications of HLA-DR expression, have been demonstrated in thymoma thymocytes (*5,6*). Furthermore, polyclonal rearrangements of T-cell receptor (TCR) genes and cytoplasmic expression of TCR molecules have been found (*7*). Immunohistochemical studies have also shown the presence of cell subsets containing neuropeptide hormones including substance P, bombesin, and so on, in the cortical areas of normal thymus, as well as in thymomas, suggesting that neoplastic cells are derived from a common epithelial stem cell capable of both cortical and subcapsular differentiation (*8*). Similar examples of heterogeneity have been reported for leukemia and epithelial tumors, in which different cell types derivate by a common ancestor cell (*9,10*). The influence of neuropeptides on immune functions and their growth-promoting activity on epithelial and mesenchimal cells suggests a potential modulatory role for peptide molecules in the biological behavior of tumors including thymomas (*11,12*).

The thymus can be considered a major neuroendocrine gland, which secretes a heterogeneous family of polypeptide hormones. These hormones regulate the immune system (inducing the proliferation and differentiation of T lymphocytes) and the neuroendocrine system (*13*). Thymic hormones' secretion is under the control of other hormones (i.e., thyroid hormones, prolactin, adrenocorticotropic hormone, opioids and so on), which have specific receptors on the surface of thymocytes (*13*). A normal thymus in children or adults expresses high densities of somatostatin receptors (SRs) within the medullae, with a lack of expression in the cortex and Hassal's corpuscles, as shown by autoradiography with [^{125}I]-Tyr^3-octreotide (*13*). The homogeneous binding of this ligand to the histologic sections and the intrinsic limits of autoradiography did not allow precise definition as to which cell type(s) in the thymic medullae express SRs (vascular epithelial cells, stroma, reticulo-endothelial cells or lymphocytes). SRs were also found in thymic carcinoids, whereas they were not measurable in the four tested thymomas (*13*). This result is in contrast with the principle that malignancies originating from tissue SRs positive express high amounts of receptors (*14,15*). Furthermore, in none of the large series of patients imaged with [^{111}In-DTPA-D-Phe^1]-octreotide, uptake within the normal thymus has been reported (*14,16*).

Because the thymus is a neuroendocrine gland and [^{111}In-DTPA-D-Phe^1]-octreotide showed an elevated diagnostic accuracy in localizing neuroendocrine as well as non-neuroendocrine tumors, we investigated the potential role of this scintigraphy in detecting and characterizing thymic masses (*14,16–25*). Furthermore, the ability of [^{111}In-DTPA-D-Phe^1]-octreotide in selecting those patients who might benefit from treatment with octreotide, which inhibits the secretion of tumor-growth factors and exerts antiproliferative effects per se (*26,27*), might have a significant relevance in thymoma, for which therapeutic options are not well categorized.

Received Dec. 18, 1996; revision accepted Jul. 16, 1997.

For correspondence or reprints contact: Secondo Lastoria, MD, Via Modigliani 66/68, Aversa (CE), 81031, Italy.

TABLE 1
Patient Profiles at Study Entry

Patient no.	Sex	Age (yr)	Histologic diagnosis/clinical suspicion	Known sites of disease	Tumor size (cm)*	Associated symptoms	Previous therapies
1	F	26	Mixed thymoma prevalent epithelial cellular component	Right lung metastasis (medial lobe)	2.5 × 2	Hyperprolactinemia	Surgery; chemotherapy
2	F	29	Mixed thymoma prevalent lymphoid cellular component	Remnant tumor Right lung metastasis (upper lobe) Pleural nodules	4.5 × 2 2.3 × 2 1 × 1.5	Myastenia	Surgery; chemotherapy; radiotherapy
3	F	57	Mixed thymoma prevalent epithelial cellular component	Mediastinal mass	13 × 8	PRCA	Mediastinoscopy; chemotherapy
4	F	50	Thymic carcinoma prevalent epithelial cellular component	Mediastinal mass infiltrating great vessels; pleural effusion	8 × 6	Dyspnea	Toracothomy
5	M	18	Thymic carcinoid	Mediastinal mass	5.5 × 5	Dyspnea/Pain; elevated calcitonin	Tracheotomy; chemotherapy
6	F	52	Mixed thymoma prevalent epithelial cellular component	Lower mediastinal mass	4.2 × 2.8	Myastenia	Biopsy
7	F	37	Suspected thymoma	Mediastinal mass Pleural metastases	8 × 7.5 2 × 1.2	Dyspnea	None
8	F	54	Suspected thymoma	Mediastinal mass	4 × 3.2	Myastenia	None
9	F	33	Suspected thymoma	Mediastinal mass Right lung metastasis Left lung	4 × 3 3.6 × 2 2 × 1.8	Dyspnea	None
10	M	36	Suspected thymoma	Mediastinal mass	4 × 3	Myastenia	None
11	F	50	Thymic carcinoma	Mediastinal mass, highly undifferentiated	5 × 7 Lung metastases	Chest pain NM	Surgery; chemotherapy; radiotherapy
12	F	38	Suspected thymoma	Mediastinal mass	2 × 2.8	Myastenia	None
13	M	61	Suspected thymoma	Mediastinal mass	3 × 2	None	None
14	M	78	Suspected thymoma	Mediastinal mass	6 × 3.5	Dyspnea	None
15	F	54	Suspected thymoma	Mediastinal mass	NM	Myastenia	None
16	F	38	Suspected thymoma	Mediastinal mass	NM	None	None
17	M	22	Suspected thymoma	Mediastinal mass	3.5 × 2	Myastenia	None
18	F	56	Suspected thymoma	Mediastinal mass	NM	None	None

*Tumor size measured by CT and/or MRI.
PRCA = pure red cell aplasia; NM = not measured.

MATERIALS AND METHODS

Patients

Eighteen patients (13 women, 5 men; ages 18–78 yr) with histologically proven (n = 7) or high suspicion of thymoma (n = 11) were enrolled in this protocol. Patients, being aware of the experimental nature and the relative lack of risks of the procedure, gave informed consent to participate in the study. Patient data are shown in Table 1. At study entry, one patient (Patient 1) had a total tumorectomy and two (Patients 2 and 11) had a near-total tumorectomy because of the adherences of thymoma with adjacent anatomical structures (pleura and superior cava vein). Thus, to treat the remnant tumor, both underwent systemic chemotherapy associated with external beam radiotherapy.

In four patients (Patients 3–6), surgery was not performed because of tumor size or lack of integrity of the capsula and/or diffuse invasion of surrounding tissues. However, in these patients, needle surgical biopsies from the tumors were taken during mediastinoscopy or thoracothomy and histology was performed. In the remaining 11 patients, surgery was done after scintigraphy and routine diagnostic work-up. The work-up included chest radiography, CT, MRI and biochemical assay of selected serum tumor markers or hormones {i.e., cancer antigen 125 [CA125, normal values (n.v.) = 0–35 units/ml], neuron-specific enolase (NSE, n.v. = 0–12 μ/liter), tissue polypeptide antigen (TPA, n.v. = 0–100 units/ml), calcitonin (Ct, n.v. $\leq$ 10 pg/ml) and prolactin (hPRL, n.v. = 3–15 ng/ml)}. Histologic diagnosis was made on frozen biopsies and was corroborated by immunohistochemistry and electron microscopy analysis. Tumor staging was done according to the criteria adopted by Wang, who considers Stage I non-invasive and Stages II-IV invasive thymomas (*28*). Each patient received approximately 111 MBq of [^{111}In-DTPA-D-Phe^1]-octreotide (10 μg) by intravenous bolus injection.

Radiopharmaceutical

The somatostatin analog [DTPA-D-Phe^1]-octreotide and ^{111}In-chloride (In-Cl_3) were purchased from Mallinckrodt (Petten, The Netherlands). Peptide labeling and quality control procedures were performed in our radiopharmacy according to the manufacturer's recommendations. The labeling yield was higher than 97% in injected preparations.

Imaging Procedure

Scintigraphic studies were performed using a large field of view rotating gamma camera (Orbiter II, Siemens, Erlangen, Germany) equipped with a medium-energy collimator. Photopeaks were set at

172 and 247 keV with a 20% window. Images were stored in a dedicated computer (Microdelta, Siemens). The images were collected at 3–4 and 24 hr after injection. Anterior and posterior whole-body images (20 min; 128 × 128 size matrix) were acquired after bladder voiding. Spot views of the head, chest and abdomen/pelvis were acquired for 10 min or 600 kcts, whichever occurred first. The emission timings were 3–4 hr and 24 hr after injection. SPECT images of the chest were obtained in 16 patients at the same time as the planar views using a step-and-shoot procedure. The orbit was elliptical over 360°. Sixty-four images (64 × 64 size matrix) were gathered every 5° and 6 min for 40–60 sec. Reconstructions were performed using a Hamming filter (frequency cutoff = 0.5 cycles/cm) before filtered backprojection with a ramp filter and no attenuation correction. Three-pixel-thick transaxial, coronal and sagittal tomograms were created.

Image Analysis

Irregular regions of interest (ROIs) delineating the tumor and the background (lung) were manually drawn by two experienced nuclear medicine physicians. For each lesion, the uptake index was determined by dividing the average counts/pixel within a lesion over the average counts/pixel in normal tissues. This method was used to minimize the heterogenity of [^{111}In-DTPA-D-Phe^{1}]-octreotide uptake within lesions.

MRI

MRI studies were performed in 12 patients using a 1.5 Tesla machine (Magnetom, Siemens, Erlangen, Germany). T1 (TR 600; TE 15) and T2 (TR 2000, TE 15–90) spin-echo sequences were acquired in the three orthogonal planes, 8-mm thick slices, before and after intravenous injection of Gd-DTPA (Magnevist, Schering, Berlin, Germany, 0.5 *M*/liter; 0.2 ml/kg of body weight).

RESULTS

Pathologic and Clinical Findings

Histologic and electron microscopy findings diagnosed mixed epithelial/lymphoid thymoma in 10 patients (Patients 1–3, 6–10, 12 and 13), carcinoma in 2 (Patients 4 and 11), carcinoid in 1 (Patient 5), lymphangioma in 1 (Patient 14) and benign follicular thymic hyperplasia in four patients (Patients 15–18). The diagnosis of thymic tumors was known at study entry for seven patients (Patients 1–6 and 11), whereas it was obtained after SRS in 11. Two thymomas were Stage I, three were Stage II, two were Stage III and six were Stage IV.

In seven patients (Patients 2, 6, 8, 10, 12, 15 and 17), myasthenia was the presenting symptom. In a 50-yr-old woman (Patient 3), thymoma was associated to pure red cell aplasia (PRCA). In a 26-yr-old woman (Patient 1), metastatic thymoma was associated with hyperprolactinemia. The thymic carcinoid was characterized by increased levels of calcitonin (Patient 5). In Patients 3, 4, 7, 9 and 11, elevated CA-125 levels (range 47–236 units/ml) were found.

CT and MRI

CT was used to determine the morphology and extent of the lesions. In seven patients, a well-defined mass occupying the upper anterior mediastinum was detected with diameters ranging between 2 × 2.8 and 4.2 × 2.8 cm. In three women (Patients 15, 16 and 18), an enlargement of the upper mediastinum was noticed. In six patients, the presence of intrathoracic metastases was documented, and calcifications, missed by MRI, were detected in two large masses. Cysts and/or areas of necrosis were found in the two patients with the largest tumors. Pleural effusions were demonstrated in five patients.

MRI was performed in 12 of 18 patients. Six large masses were plurilobulated. The lobules were divided by well-defined fibrous septa, as shown in Figure 1. Five lesions appeared well-capsulated, and one had infiltrated the muscles of the neck.

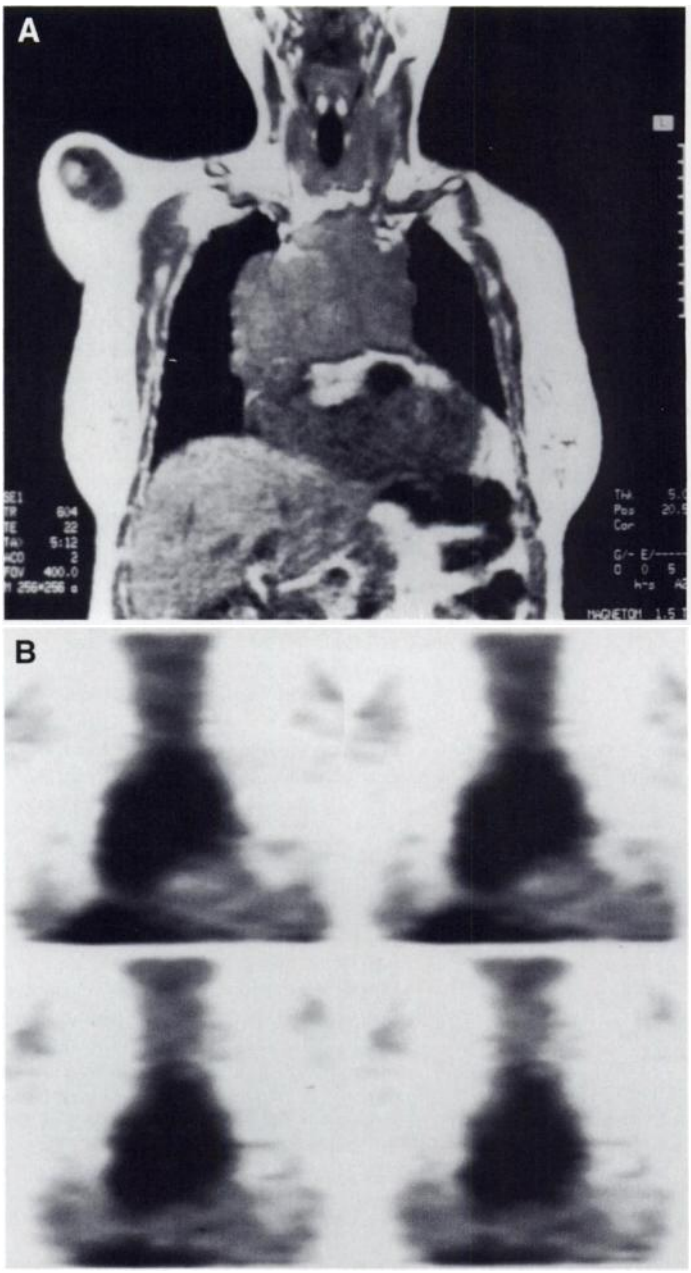

FIGURE 1. MRI T1-weighted images of Patient 2. (A) Coronal image clearly delineates tumor extent and anatomical boundaries. The structure is characterized by several lobules well-defined by fibrous septa. This finding is commonly described in aggressive thymomas. (B) SPECT with [^{111}In-DTPA-D-Phe^{1}]-octreotide: coronal views show intense tracer accumulation in the thymoma.

Signal intensity was unable to differentiate thymic hyperplasia (Patients 15 and 17) from early thymoma stages (Patients 6, 10, 12 and 13), and surgical biopsy was required for the final diagnosis in these patients.

SRS

Primary and metastatic intrathoracic thymoma deposits that were greater than 1.5 cm were clearly detected by planar scintigraphy either at 4 or 24 hr. Conversely, in two patients, small pleural and pericardial metastatic implants, detected either by CT and/or MRI, were missed by SRS. The T/L ratios 24 hr postinjection were slightly increased or were identical to those measured at 3–4 hr. We analyzed these latter values, which are listed, patient by patient, in Table 2. A wide range of

TABLE 2
Summary of Histologic and SRS Results

Patient no.	Histology	SRS (MBq/μg)	SRS Results	SRS T/L ratios
1	Mixed thymoma (>E)	95.4/10	Positive	1.7
2	Mixed thymoma (>L)	99.5/10	Positive	1.8
				1.8
3	Mixed thymoma (>E)	102/10	Positive	3.2
4	Thymic carcinoma (>E)	101/10	Positive	7.6
5	Thymic carcinoid	108/10	Positive	2.2
6	Mixed thymoma (>E)	100/10	Positive	3.1
7	Mixed thymoma (>E)	111/10	Positive	2.4
				NV
8	Mixed thymoma (>L)	105/10	Positive	4.6
9	Mixed thymoma (>E)	106/10	Positive	4.0
				NV
10	Mixed thymoma (>E)	92.4/10	Positive	5.2
11	Mixed thymoma (>E)	106/10	Positive	4.5
12	Mixed thymoma (>E)	101/10	Positive	4.1
13	Mixed thymoma (>E)	106/10	Positive	3.7
14	Lymphangioma	110/10	Negative	NM
15	Thymic hyperplasia	110/10	Negative	NM
16	Thymic hyperplasia	98/10	Negative	NM
17	Thymic hyperplasia	105/10	Negative	NM
18	Thymic hyperplasia	104/10	Negative	NM

T/L = tumor-to-lung ratio; >E = prevalent epithelial; >L = prevalent lymphoid component; NV = not visualized; NM = not measured.

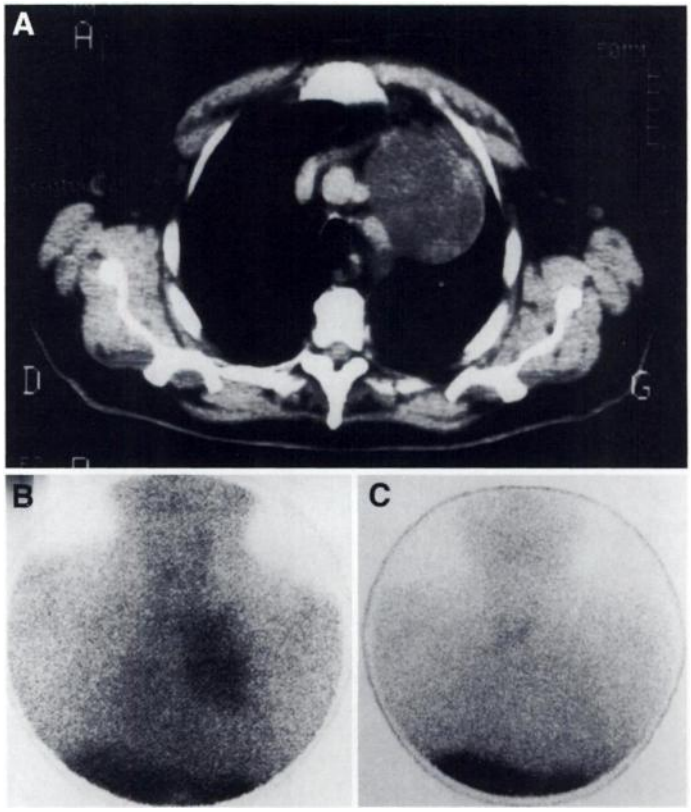

FIGURE 3. (A) CT scan after contrast enhancement in a patient with lymphangioma accurately defines the extent of the tumor mass involving the upper anterior mediastinum and the upper lobe of the left lung. Heterogeneity within the tumor mass is accurately defined by the different densitometric measurements, with a necrotic area surrounded by viable neoplastic tissue. (B) Anterior view of the chest 4 hr after [^{111}In-DTPA-D-Phe^1]-octreotide administration shows peptide uptake within the lesion. (C) There is no tracer accumulation in the 24-hr images.

T/L was observed (1.7–7.6-fold). A statistically significant difference was observed in the T/L ratios measured in untreated versus previously treated patients ($p < 0.05$). In untreated patients, the mean ratio was 4.34 ± 1.57. In treated patients, it was 2.68 ± 1.18. In two patients, pulmonary and pleural metastases, although clearly targeted, had T/L ratios of <2-fold. This was not a common finding. In fact, in a third patient with advanced metastatic malignant thymoma, T/L ratios were as high as 4.5-fold (Fig. 2). No correlations were found between tumor uptake and size. Large masses concentrated [^{111}In-DTPA-D-Phe^1]-octreotide more than small lesions with higher T/L ratios (i.e., Patients 4 and 11). Two large thymic carcinomas showed the highest T/L ratios in our series, even greater than that measured in the thymic carcinoid.

The behavior of [^{111}In-DTPA-D-Phe^1]-octreotide was completely different in the patient with lymphangioma. Tracer accumulation was seen at 4 hr in the CT-documented lesion (Fig. 3). Late images at 24 hr did not confirm the early scans with a lack of ligand accumulation. This case was initially considered negative. After histology, it was classified as true-negative.

SPECT studies were performed in 16 patients because the other two had significant thoracic pain and could not stand motionless for the entire acquisition. SPECT reconstructions more precisely delineate tumor extent than do planar views. The

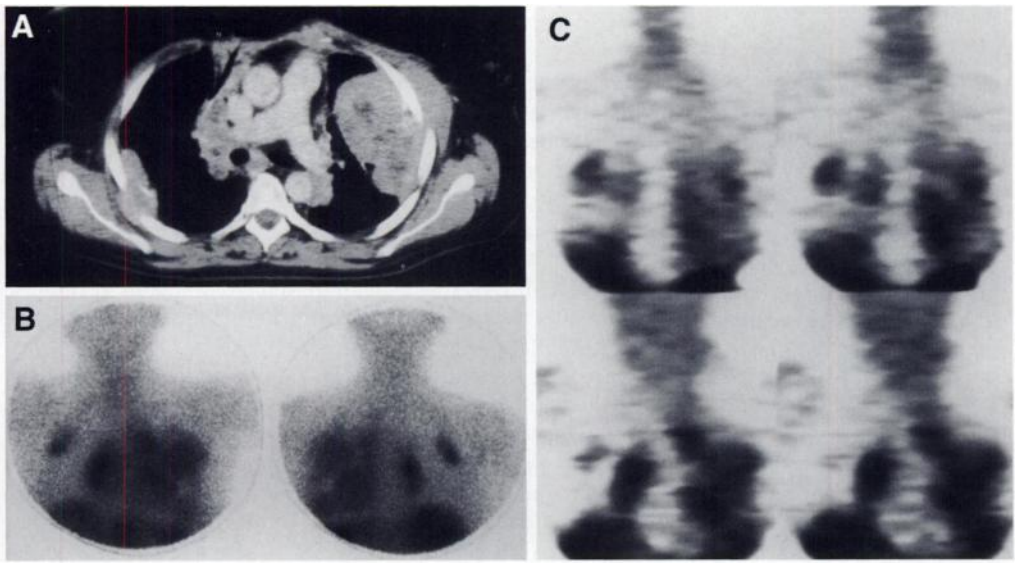

FIGURE 2. (A) Multiple bilateral pulmonary and pleural thymoma metastases are clearly detected by anterior and posterior views 24 hr postinjection. (B) The CT slices confirm the sites of disease documented by SRS. (C) Coronal tomographic slices acquired at 24 hr.

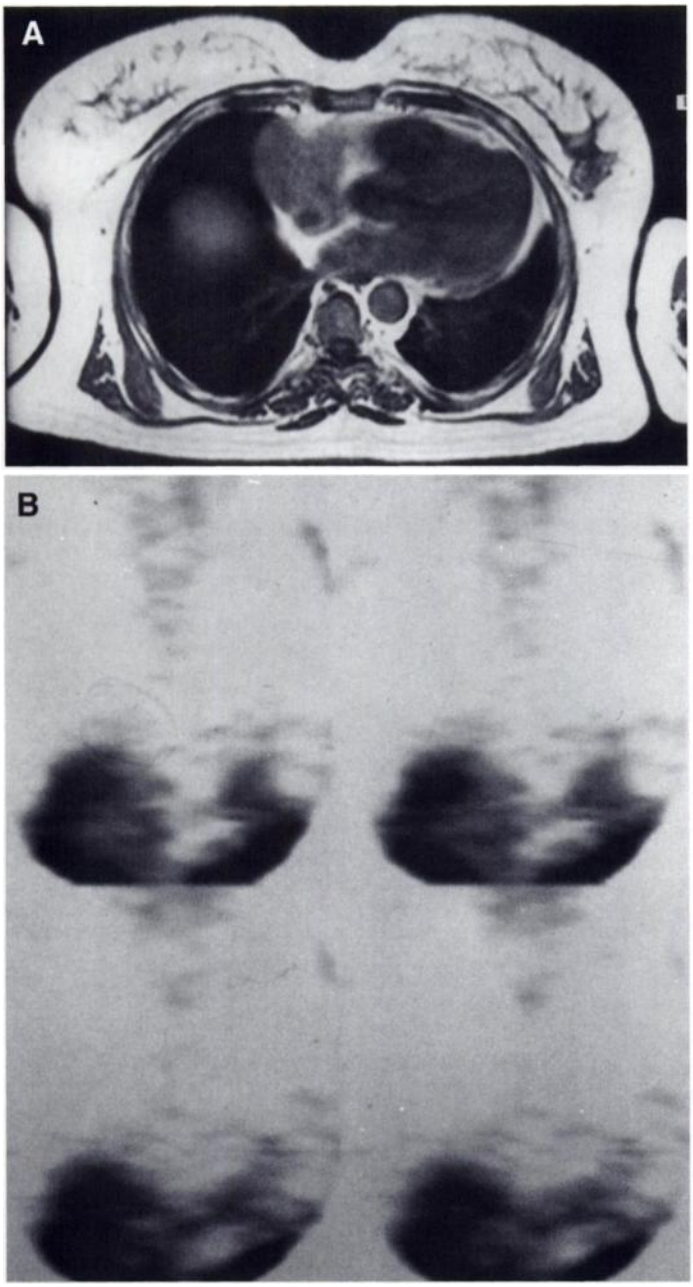

FIGURE 4. (A) Transaxial MR image showing a well-capsulated mass of the anterior mediastinum. (B) Coronal SPECT views indicate lack of [^{111}In-DTPA-D-Phe^1]-octreotide accumulation in the mass. Histologic diagnosis was thymic hyperplasia.

involvement of adjacent anatomical structures (i.e., great vessels) was identified in photopenic areas. SPECT studies did not improve the rate of tumor detection because they missed small pleural and pericardial nodules of ≤1.5 cm.

Thymoma was histologically proven in three of seven patients who had myasthenia gravis as a presenting symptom. The three thymic tumors showed intense [^{111}In-DTPA-D-Phe^1]-octreotide uptake; the four thymic hyperplasias did not on planar or SPECT images (Fig. 4). In two patients, benign thymic hyperplasia showed CT and MRI patterns similar to early-stage thymoma.

DISCUSSION

In this study, we have shown that [^{111}In-DTPA-D-Phe^1]-octreotide detects primary and metastatic thymoma, either previously treated or not, with the exception of small metastatic pleural and/or pericardial nodules. The degree of peptide uptake was extremely variable and poorly correlated with tumor size and histotype, clinical behavior of the disease and prognosis. The T/L ratios were higher in the thymomas with prevalent epithelial component than in those with a prevalent lymphoid component, as well as in untreated versus treated ones. The scintigraphic results and the pattern of [^{111}In-DTPA-D-Phe^1]-octreotide uptake by thymic tumors suggest expression of SR within neoplastic cells. The lack of [^{111}In-DTPA-D-Phe^1]-octreotide accumulation at 24 hr in the patient with lymphangioma seems to corroborate such hypothesis. Probably, the mild uptake seen 4 hr postinjection was more likely related to nonspecific phenomena, including increased blood flow supply to the lesion, slow tracer diffusion through the mass, and so on.

These in vivo results were unexpected. In a previous in vitro study, lack of SR was documented in four tested thymomas (*13*). On the other hand, in normal thymuses, as depicted by autoradiography, elevated SR content was shown. No evidence of [^{111}In-DTPA-D-Phe^1]-octreotide uptake has been reported in humans (*14,16–18*). The discrepancy between in vitro and in vivo results allows postulation of different hypotheses, which have to be experimentally proven. Lack of normal thymus visualization during SRS may be consequent to a slower receptor turnover in lymphatic tissues (*13*). Alternatively, but not improbably, it might be due to low in vivo sensitivity of SRS in detecting specific receptors (*13*).

Besides consideration of possible mechanism(s) regulating [^{111}In-DTPA-D-Phe^1]-octreotide uptake within thymomas, the results in this series of patients have an intriguing clinical outcome. In fact, none of the four patients with thymic hyperplasia concentrated [^{111}In-DTPA-D-Phe^1]-octreotide. This finding allowed accurate differentiation of benign follicular hyperplasia from early-stage thymoma, which is of great value in patients with myasthenia gravis. Thus, in this setting, SRS might allow overcoming the limitations encountered with both CT and MRI in this series as well as in other studies. With MRI, some peculiar aspects have been described for advanced thymomas, whereas there is no definitive evidence of signs or essays that may characterize early-stage, noninvasive thymomas (*30*).

Because there is not striking evidence of the effectiveness of radical surgery in eliminating myasthenia in patients with thymic hyperplasia and medical therapy is more effective (*31*), an imaging modality that can make a differential diagnosis is significantly helpful. In recent research to address this issue (*32*), ^{18}F-fluorodeoxyglucose PET has been proposed because it shows a significant difference in glucose consumption between malignant and benign thymic masses. In comparison, the use of SRS is less costly. However, other radiotracers may not be suitable in this setting. Iodine-131-radioiodine concentrates in thymic hyperplasia occurring in patients who had undergone previous surgery for differentiated thyroid cancer and were treated with radioiodine (*33*). Gallium-67-citrate is concentrated in thymic hyperplasia occurring in a child with non-Hodgkin's lymphoma, mimicking metastatic spread, who had been heavily treated previously (*34*). For both tracers, thymic rebound after therapy was the more likely explanation. In these latter patients, as well as the patients in our series, no evidence of [^{111}In-DTPA-D-Phe^1]-octreotide was seen.

SRS cannot substitute morphologic evaluation of thymomas, but it has to be associated to them for a more accurate characterization. In fact, accurate staging is important for selection of proper strategy, is an important prognostic factor and has a major role in the survival rates of these patients. Small pleural or pericardial nodules, clearly documented by CT and/or MRI, are missed by SRS because of size (≤1.5 cm) or are

masked by larger, adjacent tumor masses that avidly concentrate [^{111}In-DTPA-D-Phe^1]-octreotide. The use of a multimodality diagnostic approach (SRS + CT and/or MRI) in characterizing thymic masses, besides the rare incidence of the disease, does not dramatically burden treatment costs by forcing the use of only one diagnostic strategy. In addition, imaging with [^{111}In-DTPA-D-Phe^1]-octreotide might play a pivotal role in the correct identification of multiendocrine neoplasias syndromes (MEN) (*35*). In fact, it has been described that carcinoid of the thymus and thymomas may occur with either MEN type I (Werner's syndrome: pituitary, parathyroid and pancreas islet-cell tumors) or MEN type II (Sipple's syndrome: medullary thyroid cancer, pheocromocytoma and hyperparathyroidism) syndromes. Because these tumors are usually rich in SR content, they can be earlier and accurately identified.

Before this study, there was only evidence of thymic carcinoid detection by [^{111}In-DTPA-D-Phe^1]-octreotide (*36*). Thus, the knowledge that thymomas concentrate [^{111}In-DTPA-D-Phe^1]-octreotide further confirms the concept of "dispersed neuroendocrine cells" previously proposed by Pearse (*37*). In addition, positive SRS may be used to classify tumors by new criteria including cytostatic drug receptor profile and response to targeted therapy. The high uptake of [^{111}In-DTPA-D-Phe^1]-octreotide in thymomas suggests its use for treatment alone or in association with other drugs. Recently, a therapeutic approach based on the combined use of octreotide and prednisone enabled thymoma shrinkage and PRCA remission in a woman with thymoma and PRCA (*38*). This regimen opens a new horizon in the treatment of thymic malignancies and seems to be more effective than current strategies, especially in unresponsive patients.

CONCLUSION

Indium-111-DTPA-D-Phe^1-octreotide successfully images thymic malignancies, although it is not concentrated in benign thymic hyperplasia. Such evidence has a major role in differentiating and characterizing thymic masses in patients with myasthenia gravis. Finally, the degree of [^{111}In-DTPA-D-Phe^1]-octreotide uptake seems to reflect SR content in these tumors, although we do not have definitive in vitro evidence to corroborate in vivo findings.

ACKNOWLEDGMENTS

This work is part of a study supported by grants from the Italian Ministry of Health F.S.N. 93 entitled: "Characterization of Tumors Expressing Somatostatin Receptors by In Vitro and In Vivo Use of Radiolabeled Octreotide." This work was presented in part at the 41st Annual Meeting of the Society of Nuclear Medicine, June 5-8, 1994.

REFERENCES

1. Rosenberg JC. Neoplasms of mediastinum. In: De Vita VT, Hellmann S, Rosenberg SA, eds. *Cancer principles and practical oncology*, 3rd Ed. Philadelphia: J.B. Lippincott Co.; 1989:706–724.
2. Hoda SA, Warren GP, Zaman MB. Extrathoracic metastatic malignant thymoma diagnosis by aspiration cytology. *Arch Pathol Lab Med* 1991;115:399–401.
3. Rosai J, Levine GD. Tumors of the thymus. In: Rosai J, ed. *Atlas of tumor pathology*. Washington, DC: Armed Forces Institute of Pathology; 1976:1–166.
4. Chilosi M, Iannucci A, Fiore Donati L, et al. Myasthenia gravis: immunohistological heterogeneity in microenvironmental organization of hyperplastic and neoplastic thymuses suggesting different mechanisms of tolerance breakdown. *J Neuroimmunol* 1986;11:191–204.
5. Chilosi M, Iannucci A, Manestrina F, et al. Immunohistochemical evidence of active thymocyte proliferation in thymoma: its possible role in the pathogenesis of autoimmune disease. *Am J Pathol* 1987;128:464–470.
6. Janossy G, Bofill M, Trejdosiewicz LK, Willcox HNA, Chilosi M. Cellular differentiation of lymphoid subpopulations and their microenvironments in the human thymus. In: Muller-Hermelink HK, ed. *The human thymus. Histophysiology and pathology*. Berlin: Springer; 1986:89–125.
7. Scarpa A, Chilosi M, Cappelli P, et al. Expression and gene rearrangement of the T-cell receptor in human thymomas. *Virch Arch B Cell Pathol* 1990;58:235–239.
8. Lauriola L, Maggiano N, Larocca LM, et al. Cells immunoreactive for neuropeptide in human thymomas. *J Clin Pathol* 1990;43:829–832.
9. Greaves MF. Target cells, differentiation and clonal evolution in chronic granulocytic leukemia: a model for understanding the biology of malignancy In: Shaw MT, ed. *Chronic granulocytic leukemia*. New York: Praeger; 1982:15–47.
10. Pierce GB, Nakane PK, Martinez-Hernandez A, Ward JM. Ultrastructural comparison of differentiation of stem cells of murine adenocarcinomas of colon and breast with their normal counterparts. *J Natl Cancer Inst* 1977;58:1329–1345.
11. Larsson LI. Regulatory peptides and amines during ontogeny and in nonendocrine cancers: occurrence and possible functional significance. *Prog Histochem Cytochem* 1988;17:89–111.
12. Zachary J, Wol PJ, Rozengurt E. A role for neuropeptides in the control of cell proliferation. *Dev Biol* 1987;124:295–308.
13. Reubi JC, Waser B, Horisberger U, et al. In vitro autoradiographic and in vivo scintigraphic localization of somatostatin receptors in human lymphatic tissue. *Blood* 1993;82:2143–2151.
14. Lamberts SWJ, Krenning EP, Reubi JC. The role of somatostatin and its analogues in the diagnosis and treatment of tumors. *Endocrinol Rev* 1991;12:450–482.
15. Reubi JC, Laissue J, Krenning EP, Lamberts SWJ. Somatostatin receptors in human cancer: incidence, characteristics, functional correlates and clinical implications. *J Steroid Biochem Mol Biol* 1992;43:27–35.
16. Krenning EP, Kwekkeboom DJ, Bakker WH, et al. Somatostatin receptor scintigraphy with [^{111}In-DTPA-D-Phe^1]- and [^{123}I-Tyr^3]-octreotide: the Rotterdam experience with over 1000 patients. *Eur J Nucl Med* 1993;20:716–731.
17. Krenning EP, Bakker WH, Breeman WAP, et al. Localization of endocrine-related tumors with radioiodinated analogue of somatostatin. *Lancet* 1989;i:242–244.
18. Lamberts SWJ, Bakker WH, Reubi JC, et al. Somatostatin receptor imaging in the localization of endocrine tumors. *N Engl J Med* 1990;323:1246–1249.
19. Lamberts SWJ, Chayvialle JA, Krenning EP. The visualization of gastroenteropancreatic endocrine tumors. *Metabolism* 1992;9(suppl 2):111–115.
20. Jamar F, Fiasse R, Leners L, Pauwels S. Somatostatin receptor imaging with In-111 pentetreotide in gastroenteropancreatic neuroendocrine tumors: safety, efficacy and impact on patient management. *J Nucl Med* 1995;36:542–549.
21. Kwekkeboom DJ, Kho GS, Lamberts SWJ, et al. The value of octreotide scintigraphy in patients with lung cancer. *Eur J Nucl Med* 1994;21:1106–1113.
22. Flamen P, Bossuyt A, de Greve J, Pipeleers-Marichal M, Keuppens F, Somers G. Imaging of renal cell cancer with radiolabeled octreotide. *Nucl Med Commun* 1993;14:873–877.
23. Vanhagen PM, Krenning EP, Reubi JC, et al. Somatostatin analogue scintigraphy of malignant lymphoma. *Br J Haematol* 1993;83:75–79.
24. van Eijck CH, Krenning EP, Bootsma A, et al. Somatostatin receptor scintigraphy in primary breast cancer. *Lancet* 1994;343:640–643.
25. Lee JD, Kim DI, Lee JT, Chang JW, Park CY. Indium-111-pentetreotide imaging in intra-axial brain tumors: comparison with thallium-201 SPECT and MRI. *J Nucl Med* 1995;36:537–541.
26. Setyono-Han B, Henckelman MS, Foekens JA, Klijn JGM. Direct inhibitory effects of somatostatin (analogues) on the growth of human breast cancer cells. *Cancer Res* 1987;47:1566–1570.
27. Reubi JC, Landolt AM. The growth hormone responses to octreotide in acromegaly correlate with adenoma somatostatin receptor status. *J Clin Endocrinol Metab* 1991;68:844–850.
28. Wang LS, Huang MH, Lin TS, Huang BS, Chien KY. Malignant thymomas. *Cancer* 1992;70:443–450.
29. Moina PL, Siergel MJ, Glazer HS. Thymic mass on MR imaging. *Am J Roentgenol* 1990;155:495–500.
30. Sakai F, Sine S, Kiyono K, et al. MR imaging of thymoma: radiologic-pathologic correlation. *Am J Roentgenol* 1992;158:751–756.
31. Batra P, Hermann C Jr, Mulder D. Mediastinal imaging in myasthenia gravis: correlation of chest radiography, CT, MR and surgical findings. *Am J Roentgenol* 1987;148:515–519.
32. Lin RS, Yeh SH, Huang MH, et al. Use of fluorine-18 fluorodeoxyglucose positron emission tomography in the detection of thymoma: a preliminary report. *Eur J Nucl Med* 1995;22:1402–1407.
33. Michigishi T, Mizukami Y, Shuke N, et al. Visualization of the thymus with therapeutic doses of radioiodine in patients with thyroid cancer. *Eur J Nucl Med* 1993;20:75–79.
34. Rettenbacher L, Galvan G. Differentiation between residual cancer and thymic hyperplasia in malignant non-Hodgkin's lymphoma with somatostatin receptor scintigraphy. *Clin Nucl Med* 1994;19:64–65.
35. Pearse AGE. The cytochemistry and ultrastructure of polypeptide hormone producing cells of the APUD series and the embryologic, physiologic and pathologic implication of the concept. *J Histochem Cytochem* 1969;17:303–312.
36. Krenning EP, Kwekkeboom DJ, Oei HY, et al. Somatostatin receptor scintigraphy in carcinoids, gastrinomas and Cushing's syndrome. *Digestion* 1994;55(suppl. 3):54–59.
37. Ballard HS, Frame B, Hartrock RJ. Familial multiple endocrine adenoma-peptic ulcer complex. *Medicine* 1964;43:481–516.
38. Palmieri G, Lastoria S, Colao A, et al. Successful treatment of a patient with malignant thymoma and pure red cell aplasia with octreotide and prednisone. *N Engl J Med* 1997;336:263–265.